Supporting Information

Gao and Zhen 10.1073/pnas.1012346108

SI Materials and Methods

Strains and Culturing Conditions. The following strains were used in this study: N2 Bristol as WT, MT1212 *egl-19(n582) IV*, DA1006 *egl-19(ad1006) IV*, DA695 *egl-19(ad695) IV*, CB55 *unc-2(e55) X*, JD21 *cca-1(ad1650) X*, ZM1659 *nca-2(gk5) X;nca-1(gk9) IV*, CB251 *unc-36(e251) III*, VC550 *tag-180(ok779) II*, RB1144 *shl-1 (ok1168) IV*, RB1392 *shk-1(ok1581) II*, NM1968 *slo-1(js379lf) V*, CX3933 *slo-1(ky389) V*, LY100 *slo-2(nf100) X*, CB1091 *unc-13 (e1091) I*, ZX460 *zxIs6* [*Punc-17::ChR2(H134R)::YFP; lin-15*$^+$] *IV*, and ZX426 *zxIs3* [*Punc-47::ChR2(H134R)::YFP; lin-15*$^+$]. All strains were outcrossed against N2 at least twice. All strains were obtained from the *Caenorhabditis* Genetics Center (University of Minnesota, Minneapolis, MN) with the exception of *zxIs6* and *zxIs3*, which were received from A. Gottschalk (Goethe University, Frankfurt, Germany). All strains were cultured at 22 °C on nematode growth medium (NGM) plates seeded with OP50 unless specified otherwise (1). *zxIs6* and *zxIs3* were cultured in the dark at 22 °C on OP50-seeded NGM plates supplemented with *all-trans* retinal as described previously (2).

Electrophysiology. Recordings from dissected *C. elegans* body wall muscles were performed as described previously (3) but with modified recording solutions (see below). Briefly, 1-d-old hermaphrodite adults were glued to slides, and the body wall muscles were exposed by lateral excisions. The integrity of the anterior ventral body muscle and the ventral nerve cord were visually examined via differential interference contrast microscopy, and muscle cells were patched with fire-polished 4- to 6-MΩ resistant borosilicate pipettes (World Precision Instruments). Membrane currents and membrane potentials were recorded in the whole-cell configuration by a Digi-Data 1440A and a MultiClamp 700A amplifier using the Clampex 10 software, and data were processed with Clampfit 10 (Molecular Devices). Data were digitized at 10–20 kHz and filtered at 2.6 kHz. Cell resistance and capacitance were determined with Clampex (Molecular Devices) by applying a 10-mV depolarizing pulse with a holding potential of −60 mV, which was used to calculate the density of Ca^{2+} and K^+ currents (pA/pF). Leak currents were not subtracted.

Light stimulation of *zxIs6* and *zxIs3* was performed with an LED lamp (KSL-70; RAPP OptoElectronic) at a wavelength of 470 nm (8 mW/mm^2), controlled by the Axon amplifier software. Videos were recorded with a CCD digital camera (Zeiss Axiocam or Hamamatsu C2400) at 200 ms per frame. Simultaneous recordings of the muscle contraction and spiking activity were performed. Solution exchange was driven by gravity and completed in 5 s. All experiments were performed at room temperatures (20–22 °C).

Recording Solutions. For recording membrane potentials and K^+ currents, the pipette solution contained (in mM): 115 K-gluconate; 25 KCl; 0.1 $CaCl_2$; 5 $MgCl_2$; 1 BAPTA; 10 Hepes; 5 Na_2ATP; 0.5 Na_2GTP; 0.5 cAMP; 0.5 cGMP, pH 7.2, with~320 mosM KOH. cAMP and cGMP were included to maintain the activity and longevity of the preparation. The extracellular solution consisted of (in mM): 150 NaCl; 5 KCl; 5 $CaCl_2$; 1 $MgCl_2$; 10 glucose; 5 sucrose; 15 Hepes, pH 7.3 with ~330 mosM NaOH. For 0 Ca^{2+} extracellular solution, $CaCl_2$ was substituted with 5 mM $MgCl_2$ and 1 mM EGTA. For 0 Na^+ solutions, external Na^+ was replaced with the large cation *N*-methyl-D-glucamine ($NMDG^+$) or $Tris^+$. For recording voltage-dependent Ca^{2+} currents, the pipette solution contained (in mM): 140 CsCl; 10 TEA-Cl; 5 $MgCl_2$; 5 EGTA; 10 Hepes, pH 7.2, with ~320 mosM CsOH. The extracellular solution contained (in mM): 140 TEA-Cl; 5 $CaCl_2$; 1 $MgCl_2$; 3 4-aminopyridine ; 10 glucose; 5 sucrose; 15 Hepes, pH 7.4, with ~330 mosM CsOH. Chemical regents and blockers were obtained from Sigma unless stated otherwise.

Thrashing Assay for Body Bends in Liquid and Movement Analysis on NMG Plates. Standard thrashing assays were performed to compare the frequency of body muscle contractibility of WT and mutant animals. Individual young adult animals (24 h after L4) were transferred into a drop of 20 μL M9 buffer. After 1 min, the number of thrashes was recorded for 1 min and counted manually. A single thrash is defined as a complete sinusoidal movement through the head and tail.

For movement analysis on plates, 1- to 2-min videos of young adult stage animals crawling on the OP50-seeded NGM plates were recorded with a standard digital camera installed on a Leica MS5 dissecting microscope. Images were sampled from the videos at 1 frame per s and processed by in-house–developed ImageJ plug-ins. The longest distance of the outline of a detected object was calculated, and points giving this value were assigned as the head or tail positions. The anterior to posterior direction of the assigned points was manually determined and assigned in the first frame and tracked automatically by an in-house–developed plug-ins. The distance between the center points of the head-to-tail positions between two consecutive frames was calculated to determine the status of movement. The percentage of total frames exhibiting forward and backward movement at each pixel value was determined by using the pooled image frames from multiple animals of the same genotype.

Tissue-Specific Expression and Rescue of *egl-19(n582)*. *egl-19(n582)* mutants were injected with a DNA mix consisting of fosmid WRM0617aA03 (~2 ng/μl) that harbors the entire *egl-19* genomic region and an injection marker pTG95.62 (*sur-5::GFP*, ~15 ng/μl). Transgenic lines were selected by picking animals with bright nuclei-restricted GFP. Transgenic lines with a rescue of the sluggish locomotion, as well as defective egg-laying phenotypes exhibited by the *egl-19(n582)* mutants, were maintained to generate mosaic animals for both electrophysiology and locomotion analyses.

From the rescued transgenic Po parents, we screened for mosaic progenies that retained the transgene in either both neurons and muscles (N + M), or in neurons (N) by following GFP positive cells. Individual mosaic animals were then glued, dissected and recording, or subjected to thrashing and locomotion assays as described above.

For unknown reason, it was difficult to obtain *egl-19(n582)* mosaic animals expressing a WT EGL-19 transgene only in muscle cells (M). To generate a stable muscle EGL-19 transgene array, we isolated a 3.6-kb *egl-19* N-terminal partial cDNA fragment encoding amino acids 1–1197 of C48A7.1a by RT-PCR and cloned it into the BamHI/KpnI sites of a P*myo-3* promoter containing vector pJH580 to generate pJH2152. A 6.0-kb SalI/KpnI fragment that contains P*myo-3-egl*-19 partial cDNA fragment was purified from pJH2152 and coinjected with a fosmid WRM0620bD05, which overlaps with the last 477 bp of the Sal/KpnI fragment, along with a P*odr-1*-GFP injection marker in *egl-19(n582)* mutants. Transgenic lines were selected by picking animals with GFP-positive head sensory neurons by P*odr-1*-GFP. The proper recombination between the *Pmyo-3-egl-19* N-terminal cDNA, and the overlapping, "promoterless" *egl-19* genomic clone in transgenic lines were confirmed by PCR with a primer

pair that recognizes specifically the recombined minigene. These transgenic animals were then used for recordings and locomotion assays as described above.

Statistic Analysis. Two-tailed Student's *t* test was used to compare the difference of most datasets. $P < 0.05$ was considered statistically significant. Subsequent analysis and graphing were performed by using Excel (Microsoft), Igor Pro (Wavemetrics), and Clampfit (Molecular Devices). In this study, each cell recording is from one animal unless otherwise noted. For *egl-19(lf)*, *unc-36(lf)*, *shk-1(lf)*, and *slo-1(gf)* mutants, more than three action potentials per animal were analyzed and their mean was used as a data point for each animal, whereas more than five action potentials per animal were analyzed for WT and other mutant animals. Unless otherwise noted, data are presented as means ± SEM.

1. Brenner S (1974) The genetics of *Caenorhabditis elegans*. *Genetics* 77:71–94.
2. Liewald JF, et al. (2008) Optogenetic analysis of synaptic function. *Nat Methods* 5: 895–902.
3. Richmond JE, Jorgensen EM (1999) One GABA and two acetylcholine receptors function at the *C. elegans* neuromuscular junction. *Nat Neurosci* 2:791–797.

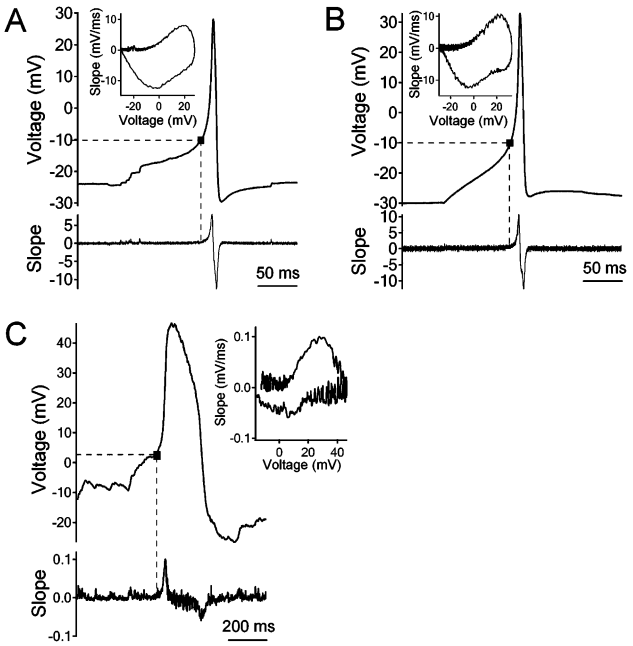

Fig. S1. Action potential threshold. (*A*) An example of spontaneous action potential by body wall muscles aligned with the derivative of action potential voltage (Slope). The action potential threshold was defined as the initial voltage after the rapid rise of action potential slope. *Inset* shows the voltage phase-plane projection (d*V*/d*t*) versus membrane potential. The dashed lines and square indicate the threshold value of the action potential. (*B*) An example of an action potential evoked by 10 pA current injection aligned with the derivative of action potential voltage (Slope). (*C*) The action potential in *egl-19(n582)* exhibited a higher threshold, which was defined and marked similarly as in *A* and *B*.

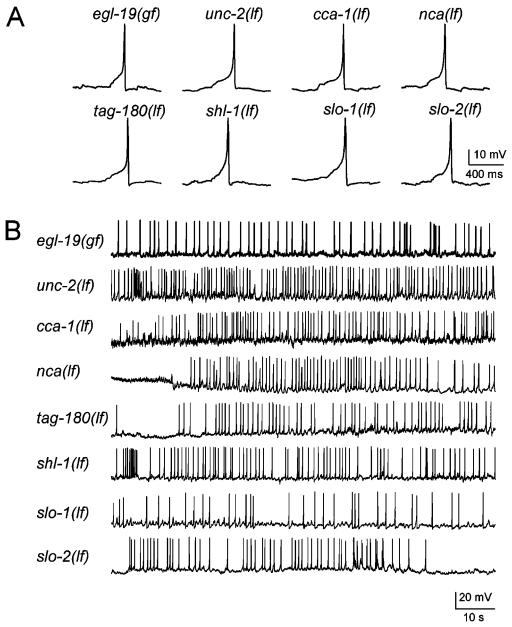

Fig. S2. The kinetics and frequency of action potentials in various channel mutants. (*A*) Representative traces for single action potentials in different mutant backgrounds. (*B*) Representative traces of spontaneous action potential trains in each mutant. Recordings were sustained for at least 100 s.

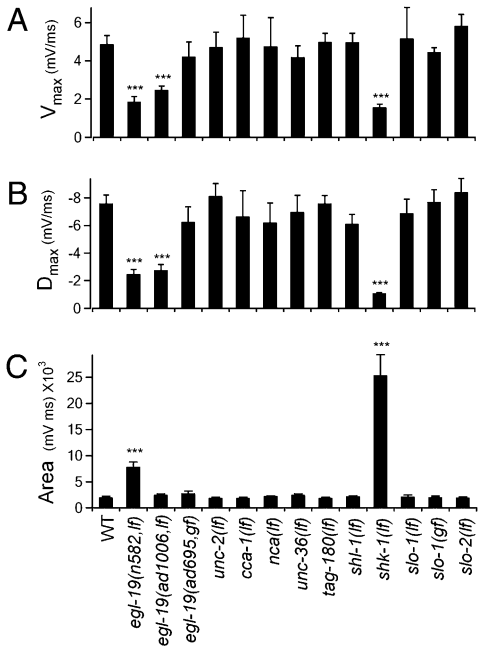

Fig. S3. Quantification of the kinetics of spontaneous action potentials in various channel mutants. (*A* and *B*) Maximum rising slope and decay slope (mV/ms) were significantly reduced in *egl-19(n582)*, *egl-19(ad1006)*, and *shk-1(lf)* mutants. (*C*) Action potential area (mV/ms) was significantly increased in *egl-19(n582)* and *shk-1(lf)* mutants. $^{**}P < 0.01$; $^{***}P < 0.001$; *t* test against WT. (Error bars = SEM.)

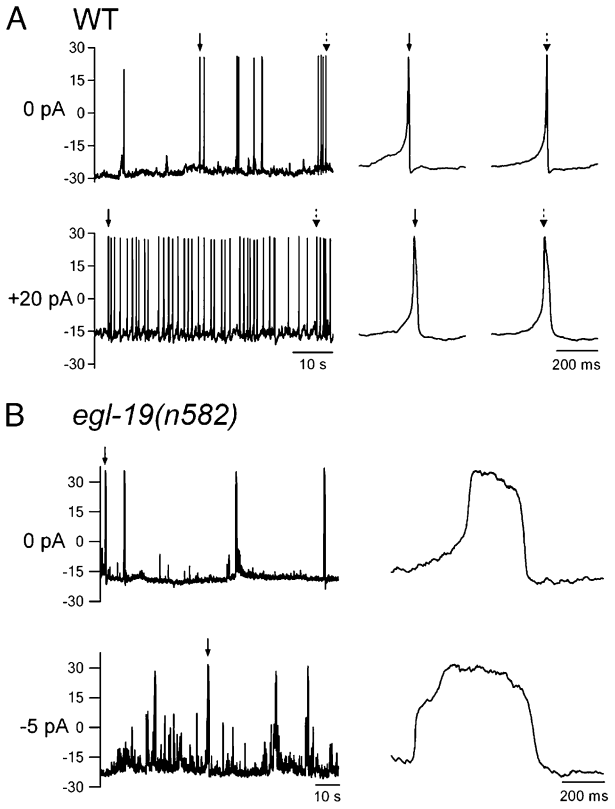

Fig. S4. Depolarizing resting membrane potential had a mild effect on action potential kinetics. (*A Upper*) Representative spontaneous action potentials firing pattern with the resting membrane potential at approximately −30 mV in WT. (*Lower*) The resting membrane potential was depolarized to −15 mV in the same muscle by +20-pA current injection. *Right* showed two single action potentials that exhibited a slightly prolonged duration and decreased amplitude at −15 mV. (*B Upper*) Representative traces of action potentials with the resting membrane potential at approximately −15 mV in *egl-19(n582)*. (*Lower*) The action potential kinetics was not restored when the membrane potential was hyperpolarized to approximately −25 mV by −5-pA current injection. *Right* showed single action potentials that exhibited a slightly prolonged duration at −25 mV.

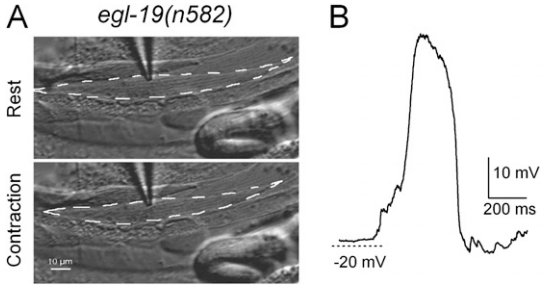

Fig. S5. Single spontaneous action potentials drove body wall muscle contractions in *egl-19(n582)* mutants. (*A*) Representative muscle morphology before (Rest) and during (Contraction) the action potential firing. (*B*) Action potentials were simultaneously recorded in the same muscle.

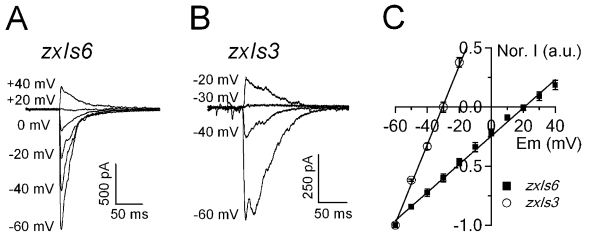

Fig. S6. Reversal potentials of ACh and GABA receptors in *C. elegans* body wall muscles. (*A*) Representative traces for currents evoked by 10-ms light stimulation at 30-s interval in *zxIs6* animals from −60 to +40 mV. (*B*) Representative traces for currents evoked by 10-ms light stimulation in *zxIs3* animals from −60 to −20 mV. (*C*) Normalized peak currents were plotted with different voltages in *zxIs6* and *zxIs3* animals. Linear fitting showed reversal potentials of +20 mV (n = 8) and −30 mV (n = 7) in *zxIs6* and *zxIs3*, respectively.

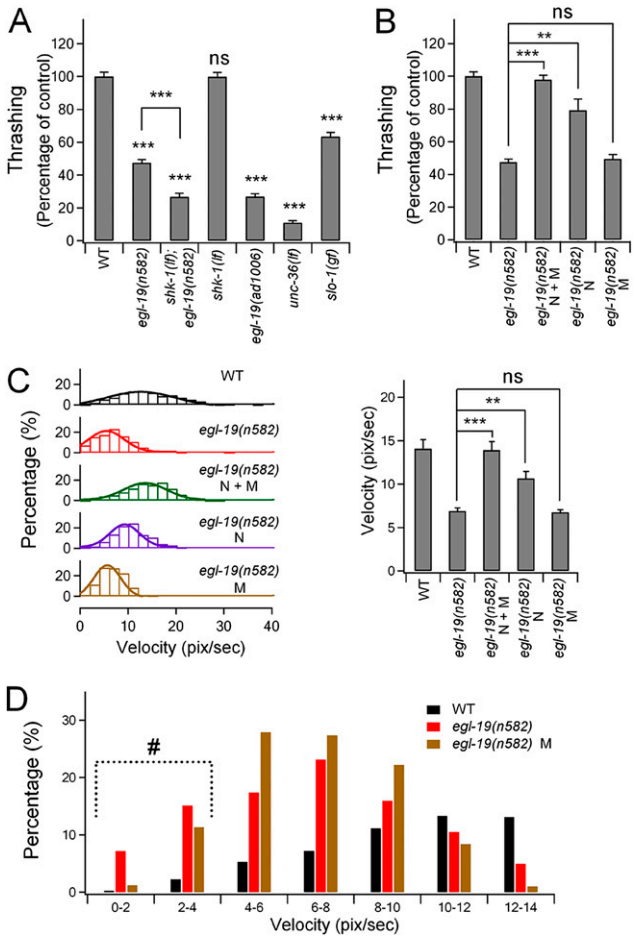

Fig. S7. Both neuronal and muscle EGL-19 expression are required to rescue the sluggishness movement of *egl-19(n582)* animals. (*A*) The frequency of body bending in M9 buffer in wild-type (WT) animals and mutants exhibiting defective action potential frequency and/or kinetics. All mutants (except *shk-1(lf)*) that affect action potential patterns showed a decreased thrashing frequency. *shk-1(lf);egl-19(n582)* double-mutant animals further enhanced the thrashing deficit of *egl-19(n582)* mutants. (n = 8 animals per genotype in each set of the thrashing assay, and the assay was repeated twice.) Asterisks denote the statistically significant difference against WT animals unless specified. (*B*) The reduced body-bending frequency of *egl-19(n582)* mutants was fully rescued in transgenic animals that expressed a functional EGL-19 transgene in both neurons and muscles (N + M), partially rescued when transgene was in neurons alone (N), and not rescued when expressed in muscles alone (M). (n = 8 animals per genotype in each set, and the experiment was repeated twice.) Asterisks represent statistically significant difference against *egl-19(n582)* animals. (*C*) The velocity of WT, *egl-19(n582)*, and *egl-19(n582)* N + M, *egl-19(n582)* N, and *egl-19(n582)* M animals on NGM plates seeded with OP50. (*Left*) The distribution (percentage of total video frames) of the speed (pixels per s) for animals of each genotype. (*Right*) The mean velocity of each genotype. The mean speed of *egl-19(n582)* N + M animals were restored to WT level, whereas *egl-19(n582)* N animals exhibited partial rescue, and *egl-19(n582)* M animals showed no statistically significant improvement in the mean velocity. (n = 360, 363, 403, 364, and 406 video frames collected from 10, 11, 11, 10, and 11 WT, *egl-19(n582)*, and *egl-19(n582)* N + M; *egl-19(n582)* N; and *egl-19(n582)* M animals, respectively. Asterisks represent statistical significance against *egl-19(n582)* animals. (*D*) *egl-19(n582)* M animals exhibited a slight improvement in speed compared with *egl-19(n582)* animals (#), although the improvement did not result in a statistically significant increase of the mean velocity. ns, not significant. $*P < 0.05$; $**P < 0.01$; $***P < 0.001$. (Error bars = SEM.)

Table S1. Summary of parameters of action potentials in different genotypes

Genotype	*n*	Channel type	Subunit	RMP, mV	Freq., Hz	Action potential kinetics					
						n	Amp., mV	Duration, ms	V_{max}, mV/ms	D_{max}, mV/ms	Area, mV/ms
WT	10			−24.5 ± 1.4	0.73 ± 0.14	8	46.0 ± 2.2	14.9 ± 1.2	4.9 ± 0.5	−7.6 ± 0.6	2,017.6 ± 184.2
egl-19(n582)IV	9	L-VGCC	α_1	−15.2 ± 1.4*	0.03 ± 0.01***	5	47.5 ± 1.3	152.1 ± 22.8**	1.9 ± 0.3***	−2.5 ± 0.4***	7,840.5 ± 949.2**
egl-19(ad1006)IV	7	L-VGCC	α_1	−25.9 ± 1.8	0.12 ± 0.03**	8	33.9 ± 2.1**	38.4 ± 5.0**	2.5 ± 0.2***	−2.8 ± 0.4***	2,464.0 ± 228.9
egl-19(ad695)IV gf	9	L-VGCC	α_1	−25.9 ± 2.6	0.75 ± 0.14	6	43.9 ± 2.9	17.8 ± 2.1	4.2 ± 0.8	−6.2 ± 1.1	2,802.2 ± 407.7
unc-2(e55)X	7	R,N,P/Q-VGCC	α_1	−23.9 ± 2.1	0.65 ± 0.10	4	45.1 ± 3.8	14.2 ± 1.5	4.7 ± 0.8	−8.1 ± 0.9	1,899.6 ± 180.2
cca-1(ad1650)X	5	T-VGCC	α_1	−23.8 ± 2.7	0.67 ± 0.13	5	44.8 ± 3.6	16.8 ± 3.0	5.2 ± 1.2	−6.6 ± 1.9	1,898.5 ± 150.3
nca-1(gk9)IV; nca-2(gk5)III	5	NALCN	α	−23.8 ± 1.0	0.78 ± 0.10	5	44.1 ± 4.1	19.8 ± 3.1	4.8 ± 1.5	−6.2 ± 1.4	2,283.2 ± 38.4
unc-36(e251)III	8	L-VGCC	$\alpha_2\delta$	−25.0 ± 2.6	0.07 ± 0.02***	6	45.5 ± 2.2	18.0 ± 2.2	4.2 ± 0.6	−7.0 ± 1.2	2,467.7 ± 197.6
tag-180(ok779)II	7	L-VGCC	$\alpha_2\delta$	−23.7 ± 2.4	0.71 ± 0.18	5	44.5 ± 1.9	14.8 ± 1.1	5.0 ± 0.5	−7.6 ± 0.6	1,892.4 ± 97.6
shl-1(ok1168)IV	6	Kv4	α	−24.8 ± 1.8	0.67 ± 0.17	8	45.3 ± 2.1	20.8 ± 2.4	5.0 ± 0.5	−6.1 ± 0.7	2,230.7 ± 110.8
shk-1(ok1581)II	15	Kv1	α	−25.1 ± 1.3	0.05 ± 0.01***	9	55.5 ± 2.2*	421.9 ± 35.8***	1.6 ± 0.2***	−1.1 ± 0.1***	25,319.8 ± 4,013.5***
slo-1(js379)V	8	BK	α	−24.3 ± 3.0	0.75 ± 0.11	3	45.9 ± 3.9	16.6 ± 4.3	5.2 ± 1.6	−6.9 ± 1.0	2,127.8 ± 343.3
slo-1(ky389)V gf	10	BK	α	−26.5 ± 2.5	0.05 ± 0.02***	6	44.2 ± 0.6	16.0 ± 1.5	4.4 ± 0.2	−7.7 ± 0.9	2,066.5 ± 187.6
slo-2(nf100)X	7	K_{Na}	α	−25.6 ± 1.7	0.76 ± 0.13	6	44.3 ± 1.6	14.4 ± 2.1	5.8 ± 0.6	−8.4 ± 1.0	1,966.6 ± 149.6

RMP, resting membrane potential; V_{max}, maximum upstroke slope; D_{max}, maximum decay slope; *gf*, gain-of-function [others are loss-of-function (*lf*) mutants]. *$P < 0.05$; **$P < 0.01$; ***$P < 0.001$; *t* test against WT. (All error bars = SEM.) Light gray shading, Ca^{2+} channels; dark gray shading, K^+ channels.

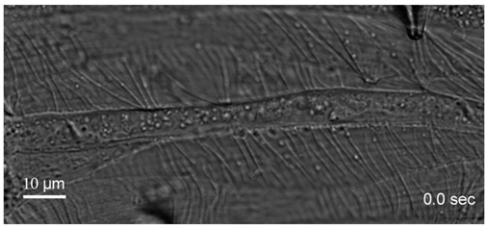

Movie S1. Muscle response in *zxIs6* (0.1 ms). A 0.1-ms light stimulation failed to induce obvious body wall muscle contractions in *zxIs6* animals.

Movie S1

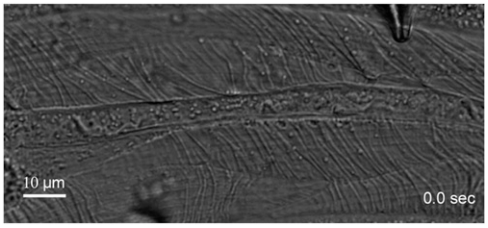

Movie S2. Muscle response in *zxIs6* (1 ms). A 1-ms light stimulation drove a brief body wall muscle contractions in *zxIs6* animals.

Movie S2

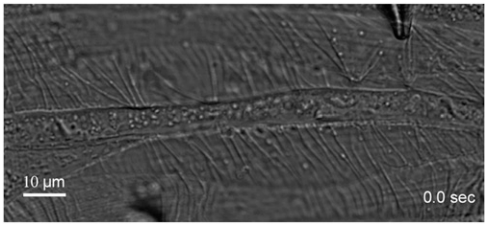

Movie S3. Muscle response in *zxIs6* (1 s). A 1-s light stimulation drove sustained body wall muscle contractions in *zxIs6* animals.

Movie S3

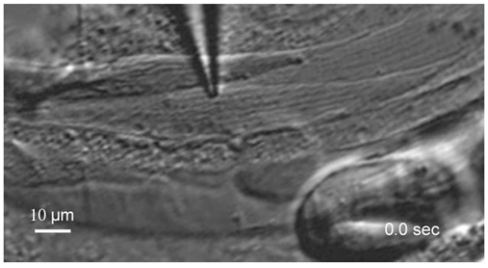

Movie S4. Muscle contraction in *egl-19(n582)*. Single spontaneous action potential drove body wall muscle contractions in *egl-19(n582)* animals.

Movie S4

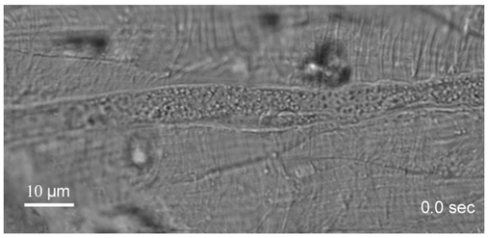

Movie S5. Muscle response in *zxIs3* (1 s). A 1-s light stimulation drove body wall muscle relaxation in *zxIs3* animals.

Movie S5